

Atmospheric observations at the Amundsen-Nobile Climate Change Tower in Ny-Ålesund, Svalbard

Mauro Mazzola¹ · Angelo Pietro Viola² · Christian Lanconelli^{1,3} · Vito Vitale¹

Received: 15 December 2015 / Accepted: 25 May 2016 / Published online: 23 June 2016
© Accademia Nazionale dei Lincei 2016

Abstract The Amundsen-Nobile Climate Change Tower (CCT) is one of the important scientific platforms operating in Ny-Ålesund, Svalbard. The CCT is equipped with a consistent set of meteorological sensors installed at different heights to provide continuous measurements of the atmospheric parameters that affect the climate and its variability. In this paper, some features of the main meteorological parameters observed during the 6 years of measurements since November 2009 are presented in order to describe the thermodynamic characteristic of the lower layers of the atmosphere and the peculiarities of CCT. Monthly and seasonal behavior of temperature, humidity and wind as well as radiation budget and albedo variability

are also shown. Such preliminary statistical description aims to provide an overview of the phenomenology occurring in the Kongsfjord area, useful to proceed with further analysis of the arctic climatic system. Even if the time series are not long enough to consider the parameters variability on a climatological time scale, useful assumptions can be made for detailed analysis concerning turbulence studies, data intercomparison at different time and space scales, validation of theory and numerical model results. CCT dataset is stored in a dedicated built-in digital infrastructure that allows other users, in the frame of international cooperations, to visualize, access and download the data and contribute to strengthen the collaboration within the scientific community operating in Svalbard.

This peer-reviewed article is a result of the multi and interdisciplinary research activities based at the Arctic Station “Dirigibile Italia”, coordinated by the “Dipartimento Scienze del Sistema Terra e Tecnologie per l’Ambiente” of the National Research Council of Italy.

Keywords Arctic · Svalbard · Meteorological vertical profiles · Radiation balance · Snow coverage and albedo · Local atmospheric circulation

✉ Mauro Mazzola
m.mazzola@isac.cnr.it

Angelo Pietro Viola
a.viola@isac.cnr.it

Christian Lanconelli
c.lanconelli@isac.cnr.it

Vito Vitale
v.vitale@isac.cnr.it

¹ Institute of Atmospheric Sciences and Climate, National Research Council, Via Gobetti 101, 40129 Bologna, Italy

² Institute of Atmospheric Sciences and Climate, National Research Council, Via Fosso del Cavaliere 100, 00133 Rome, Italy

³ Institute of Environment and Sustainability (IES), Land Resource Management Unit (LRM) H05, European Commission, Joint Research Center, 21020 Ispra, Italy

1 Introduction

The Arctic land areas are experiencing more warming than any other region on Earth (Holland et al. 2007; Serreze et al. 2009). The Arctic temperature anomalies for the most recent decade (2000–2009) reflect the combined effects of the general background warming due to Earth’s response to positive radiative forcing, to the anomalies in the atmospheric circulation, changes in characteristics of the surface, reduced sea-ice extent and increase of sea surface temperatures (Serreze et al. 2009). The coupling of the ABL with surface, besides that with the free troposphere, is one of the most important topics to be dealt with in both observations and modeling. At high latitudes ABL is often characterized by extremely stable vertical stratification.

Intensive surface radiative cooling and stable stratification forms vertical temperature inversions especially during polar night conditions over land, ice and snow surfaces (Overland and Guest 1991). Forcing factors like radiation, cloudiness, turbulence, subsidence and large-scale advection contribute to increase the complexity of the system (Boville and Gent 1998). Moreover, in the Arctic data scarcity and measuring problems are other important issues, while model results still show important deviations from observations (Moritz et al. 2002). To monitor the long-term variations of climate conditions in the Svalbard region it is important to make optimal use of observational series. Inhomogeneities over the open water surface, drifted sea ice and land determine the horizontal change of surface albedo, roughness parameter and heat flux from the surface. Difficulties in simulating the Arctic climate relate directly to an insufficient understanding of several strong feedback processes. The climate sensitivity in models is largely due to the strongly positive snow and ice albedo feedbacks that further enhance the warming, determining changes in surface heat fluxes (Curry et al. 1995; Lindsay and Zhang 2005; Screen and Simmonds 2010). As the Arctic sea ice cover is reducing faster than most of the climate models predict (Holland et al. 2007), it is necessary to ensure reliable atmospheric observation data in order to better understand the processes related to this reduction.

In this context, the Department of Earth System Science and Environmental Technologies of National Council of Research of Italy (DTA-CNR), that manages the *Dirigibile Italia Arctic Station* in Ny-Ålesund, promoted in 2009 the Climate Change Tower–Integrated Project (CCT-IP) and financially supported the construction of a 34-m tower, the Amundsen-Nobile Climate Change Tower (CCT). The aim of CCT is improve to the comprehension of the processes occurring at the interface and in the lower layers of the atmosphere by providing long time series of atmospheric profiles and physical parameters affected by the climate variability in the area.

The CCT is a unique installation in Ny-Ålesund to provide continuous observation of the atmospheric profiles that link up energy transfer processes, fluxes at the air–snow interface, energy and radiation budget at the surface, and turbulence and fine structure of ABL.

The purpose of this paper is to present the CCT scientific infrastructure by discussing the meteorological dataset to provide some information on the meteo-climatic condition in the area of Kongsfjord. In Sect. 2 a description of the site, technical details of the infrastructure and of instrumentation installed are illustrated. In Sect. 3, a preliminary statistical analysis on data collected during the measurements period 2009–2015 of the meteorological parameters, of the radiation balance and the albedo in relation with snow coverage variability are shown. Finally in Sect. 4, a

discussion on what are the peculiarities of the scientific platform for other studies of analysis, what are the links to other running research and how the complex dataset will be organized in a digital infrastructure to be accessed is presented.

2 Site and instrumentation

Ny-Ålesund is located along the coast of Kongsfjord on the west side of Svalbard, one of the northernmost archipelagos in the Arctic. The area surrounding Ny-Ålesund and Kongsfjord is characterized by a complex orography and by a unique peculiar environment (see Fig. 1). Mountains, deep valleys, glaciers, moraines, rivers, lakes and a typical tundra system can be found within few kilometers, making the site, even if a non-representative location for the Arctic in general, very important to indicate variability and change when looking at synoptic time scales and when analyzing integrated processes of the Arctic climate system (Hartmann et al. 1999). Such a complexity makes the study of the vertical structure of the ABL very challenging, in particular close to the surface. The latitudinal position of the site implies that polar night lasts between end of October and mid February while polar day between mid-April and end of August. As stated in Maturilli et al. (2013), during recent winters rain precipitation events took place very more often. Decades of meteorological data have been collected in Ny-Ålesund to analyze the climate variability in the area. Eirik et al. (2011) analyzed averaged annual and seasonal temperature recorded in Ny-Ålesund between the years 1981 and 2010, while recently Maturilli et al. (2013) provided a statistical analysis showing an increase of air temperature of 1.35 °C per decade for the years 1994–2010, while in Maturilli et al. (2015) trends in radiation regimes in the same period are shown.

With the aim of providing also vertical profiles of meteorological parameters, since October 2009 the 34-m-high meteorological tower named Amundsen-Nobile Climate Change Tower (see insert in Fig. 1) is operative in Ny-Ålesund. The location of the tower, about 2 km NW from the town and on the top of a small hill (78°55'N, 11°52'E, 50 m a.m.s.l.), has been chosen to avoid the influence of the human activity of the village and to make possible the integration with other different of measurements in the same clean and protected area.

The CCT is facing Kongsfjord that deploys along the NW and SE directions. This geographic configuration allows the prevailing wind blowing along this axis. But the surrounding area of CCT, bounded by several hills and mountains, some of them reaching thousands of meters of height like Zeppelin (475 m a.s.l.), located South with respect to the CCT, and Schetelig (694 m a.s.l.), NW of CCT, contribute to determine



Fig. 1 Map of the Brogger peninsula and of Kongsfjorden. The red dot indicates the position of the CCT, shown in the picture. Map courtesy of Norwegian Polar Institute

interesting features of the local low level of atmospheric circulation (Argentini et al. 2000).

The tower is composed by 17 aluminum modules, of sizes $1.8 \text{ m} \times 1 \text{ m} \times 1.9 \text{ m}$ height. Each module is provided with a floor to safely work on site and stairs to reach the upper modules of the tower. For every three modules a connection box for power supply and data transmission is also mounted. The data and power connection end at dedicated panels in a hut where the acquisition systems are located 30 m away from the tower in North direction. The installation of the sensors on the CCT has been done taking into account the position, the structure and the orientation of the tower itself, to reduce the environmental disturbance and get the best measurement conditions. The inspection of the instrumentation and of the tower structure is regularly performed twice a year. Four classes of instrument have been adopted: conventional meteorological, radiation budget instrument, surface sensors and fast response sensors. Detailed description of the different sensors installed on the tower is given below (see also Table 1).

2.1 Meteorological sensors

Slow response sensors, measuring at 1 Hz, were placed at four levels on the CCT (2, 5, 10 and 33 m a.g.l.). Each set includes a Vaisala thermo-hygrometer model HMP45AC, mounted in a proper shield to avoid heating by the solar

radiation, and a Young Marine wind sensor model Wind Monitor 05106. The two instruments are mounted facing North on the same arm, at about 0.5 and 1.5 m off the tower, respectively. According to the manufacturer manuals, the accuracy of the temperature measurements vary between ± 0.4 at -20 °C and ± 0.2 °C at 20 °C and that of the relative humidity measurements is ± 2 % for RH below 90 % and ± 3 % above that value. The accuracies of wind speed and direction are ± 0.3 m/s or 1 % of reading and $\pm 3^\circ$, respectively. The atmospheric pressure is measured with a Setra pressure sensor model 278 situated in the datalogger box at 5 m agl. Its accuracy is ± 0.5 hPa.

2.2 Radiation instruments

Radiation measurements are performed at two levels on the CCT to measure the radiation balance and the albedo at the top of the tower and some meters below the upward radiation fluxes, emitted and reflected, by the surface. At the top of the tower at 33.4 m, facing South on an arm stretching out 2.5 m a Kipp and Zonen net radiometer model CNR1 is installed, while at 25 m two downward-looking Kipp and Zonen first class radiometers, CM11 for SW and CG4 for LW are mounted as the CNR1. This configuration is assumed to compensate the low accuracy of 10 % of the CNR1 with respect to the accuracy of 3 % on daily totals of the higher class radiometers.

Table 1 Technical characteristics of the instrumentation installed at the CCT

Sensor	Measured parameters	Height (m)	Acquisition rate	Accuracy	Date of installation
Meteorological					
Vaisala HMP45AC thermo-hygrometer	Temperature, relative humidity	2, 5, 10, 33	1 min	$\pm 0.4\text{ }^{\circ}\text{C}$ at $-20\text{ }^{\circ}\text{C}$, $\pm 0.2\text{ }^{\circ}\text{C}$ at $20\text{ }^{\circ}\text{C}$, 2 % for RH < 90 %, 3 % for RH%>90	October 2009
Young Marine Wind Monitor 05106 anemometer	Wind speed and direction	2, 5, 10, 33	1 min	$\pm 0.3\text{ m/s}$ or 1 %, $\pm 3\text{ }^{\circ}$	October 2009
Setra 278 barometer	Pressure	5	1 min	$\pm 0.5\text{ hPa}$	October 2009
Radiation					
Kipp and Zonen CNR1 net radiometer	Incoming SW and LW radiation, surface-reflected SW and outgoing LW radiation	33	1 min	$\pm 10\%$	October 2009
Kipp and Zonen CM11 pyrgometer	Surface-reflected SW radiation	25	1 min	3% for daily total	October 2009
Kipp and Zonen CG4 pyrgometer	Outgoing LW radiation	25	1 min	3% for daily total	October 2009
Snow properties					
SR50 sonic range sensor	Snow height	2	1 min	$\pm 1\text{ cm}$	October 2009
IR120 infrared temperature sensor	Snow skin temperature	5	1 min	$\pm 0.2\text{ }^{\circ}\text{C}$	October 2009
PT100 thermistors	Snow temperature	0.05, 0.15	1 min	$\pm 0.1\text{ }^{\circ}\text{C}$	October 2009
Hukseflux HFP01 flux plate	Snow-soil heat exchange	Ground	1 min	+ 5%/-15%	October 2009
Fast response					
Gill R3 sonic anemometer	Wind components and sonic temperature	7.5	20 Hz	<1 %, <1 $^{\circ}$	March 2010
Campbell Scientific KH20 fast hygrometer	Water vapor	7.5	20 Hz	–	March 2010
Gill R2 sonic anemometer	Wind components and sonic temperature	3	20.83 Hz	<1 %, <1 $^{\circ}$	May 2012
Campbell Scientific KH20 fast hygrometer	Water vapor	3	20.83 Hz	–	May 2012
Campbell Scientific CSAT3A	Wind components and sonic temperature	20	10 Hz	–	May 2011
Campbell Scientific EC150	Water vapor and CO ₂	20	10 Hz	–	May 2011
Licor LI-7700	CH ₄	20	10 Hz	–	May 2012
LI-7500A	Water vapor	20	10 Hz	–	May 2012
Picarro CRDS	CH ₄ , CO ₂ , water vapor	20 (inlet)	–	–	May 2012

2.3 Surface instruments

The surface is monitored by a set of instruments mainly used to estimate the heat fluxes into the snow layer and between the snow layer and the soil, during the period of snow coverage. Two PT100 sensors are positioned at 5 and 15 cm above the ground while Hukseflux flux plate model HFP01 is placed on the ground to measure the snow–soil heat exchange. To complement these measurements a Campbell Scientific sonic range sensor model SR50 to measure the snow height, and a Campbell Scientific IR120 Infrared Remote Temperature Sensor to measure surface skin temperature mounted on CCT. The SR50 is mounted an arm of 1.5 m at the East side of the tower looking down from 4.30 m mounted while the IR120 is fixed on the tower at 5 m and tilted to look downward in correspondence with the snow layer sensors. Unfortunately the sensor was not operational because of some technical failures during most of 2014 and part of 2015.

2.4 Fast response sensors

To study the turbulent exchange processes between the surface and the atmosphere at the site, and establish relationships with meteorological and environmental conditions, a set of fast response sensors have been installed on CCT at three levels 3.7, 7.5 and 21 m. These sensor are mounted lined up on the same CCT upright bar of the conventional sensors. The installation that includes sonic anemometers and fast hygrometers has been done in different periods. On March 2010, a first set constituted by a Gill R3 sonic anemometer and a Campbell Scientific KH2O fast hygrometer was installed at 7.5 m. In May 2012, a Gill R2 sonic anemometer was installed 3.7 m while the corresponding KH2O fast hygrometer was installed in 2013. The two sets collect data at nominal sampling rate of 20 Hz.

At 21 m on the tower the setup concerned with a Campbell Scientific Eddy Covariance EC150 system and CSAT3A sonic anemometer owned by KOPRI was installed in 2011 in the frame of the collaboration with CNR. With the aim to deepen the study of the greenhouse gases (CO_2 , H_2O and CH_4) in May 2012, also open path gas analyzer Li-cor LI-7700 for CH_4 and CO_2 , and LI-7500 for $\text{CO}_2/\text{H}_2\text{O}$ were placed close at the sides of the Campbell installations. Furthermore, the gas inlet for a Picarro Cavity Ring-Down Spectroscopy (CRDS) gas analyzer for CH_4 and CO_2 concentration measurements was also positioned in the same place, fixing acquisition system was at the ground close to the CCT basement.

3 Data presentation and discussion

The amount of data and information does not allow to show all the measurements collected at CCT and only brief statistics of data recorded by conventional instruments during the years 2009–2015 is discussed. In particular, in the following meteorological data, the radiation measurements and some aspects of the observation at the surface during the snow coverage are shown. Further data analysis to study the interaction between the different processes are still ongoing while first results on the turbulence studies dedicated to turbulence published by Mazzola et al. (2016) and by Tampieri et al. (2016) will not be presented here.

The time interval of 1 min has been chosen to uniform different time response of sensors and from these data, basic statistics for meteorological, radiation and surface parameters were evaluated. Similar criteria of those proposed by Maturilli et al. (2013) were applied when calculating average values: hourly values were calculated only when at least 30 min of valid data were available and daily values only if less than 5-hourly not valid values were previously calculated. No discards were applied for monthly values, as few data gaps were present on the dataset. Seasonal values were also calculated, assuming the merging of the months December, January and February (DJF) for winter, March, April and May (MAM) for spring, June, July and August (JJA) for summer, and September, October and November (SON) for autumn.

3.1 Temperature, humidity and pressure

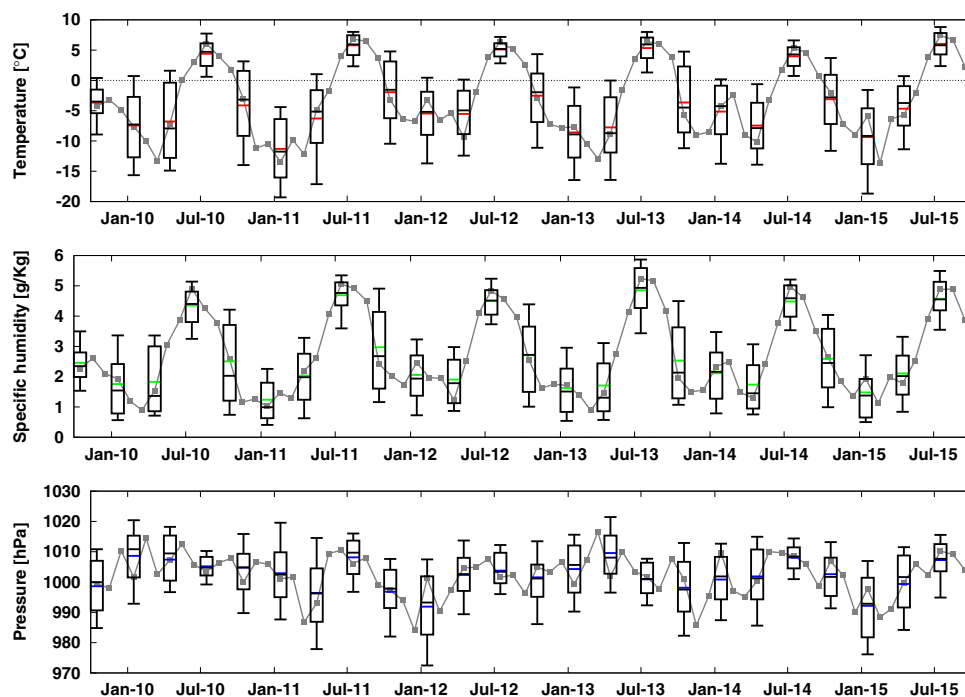
Figure 2 shows monthly means and seasonal percentiles for temperature and specific humidity measured at 2 m and pressure as measured at CCT during the years 2009–2015.

The coldest months in the winters 2010–2015 have been January 2011 with $T = -11.3^\circ\text{C}$ and February 2015 with $T = -9.4^\circ\text{C}$, but the minimum temperatures were recorded in March 2010 and 2013. Anomalous warm periods, with respect to our dataset and to data reported by Maturilli et al. (2013), were recorded during winters 2012 and 2014 with a minimum temperature of $T = -3.2^\circ\text{C}$ on January 2012 and $T = -2.4^\circ\text{C}$ on February 2014. In summer, the maximum monthly temperature ranges between 5.3°C and 7.4°C , July 2015 being the warmest summer month and July 2014 the coldest one.

The extremes of the hourly temperature were $T = -25.2^\circ\text{C}$ on February 22, 2011 and $T = 16.0^\circ\text{C}$ on August 1, 2015.

The specific humidity (SH) averaged time series measured at the CCT shows similar behavior as that of the temperature record. The minima are observed, as expected, in winter time in correspondence with air temperature minima. During the observation period the monthly

Fig. 2 Temporal evolution of monthly values and seasonal statistics for temperature (*top panel*) and specific humidity (*middle panel*) both measured at 2 m and pressure measured at 5 m (*bottom panel*). The 10th, 25th, 50th, 75th and 90th are reported, as well as the average values (*colored bars*)



averaged values varied from a minimum of 0.9 g/kg recorded in March 2013 to a maximum of 4.9 g/kg recorded in August 2013. Even if SH presented the two lowest monthly values during March, the driest season was the winter, with lowest average value of 1.2 g/kg on 2010–2011 and highest of 2.1 g/kg on 2011–2012. The highest monthly values were during July or August (4.5 g/kg $<SH < 5$ g/kg), making the summer values ranging between 4.3 g/kg on 2010 and 4.9 g/kg on 2013.

The atmospheric pressure monthly average values varied between 984 and 1017 hPa, without any evident seasonal cycle even if a possible correlation with the anomalous warm periods observed in the temperature record could be found. A high variability in terms of standard deviation can be recognized in winter season compared to summer values. As stated by Maturilli et al. (2013), this is due to the higher occurrence of cyclones with greater pressure variations.

3.2 The wind field data distribution

Due to particular orographic configuration of Kongsfjord, the wind observations in Ny-Ålesund depend on the position of the measurement site (Beine 2001). Climatological data from Norwegian Meteorological Institute, long-lasting campaigns (e.g., ARTIST, Argentini et al. 2000) and recent works (Maturilli et al. 2013) have shown that the prevalent wind comes from E-SE even if contributions to the wind distribution occur from other sectors. The site of CCT allows to observe other components of the wind field and

characterize the atmospheric flow up to 33 m above the ground level. Figure 3 shows the cumulative seasonal wind speed and direction distributions measured at 10 m for all years 2009–2015. A similar distribution, with few differences between the years (not shown) has been observed, indicating the recurrence of the average conditions. During winter, spring and autumn the direction with highest occurrence is that from E-SE, with a frequency between 15 and 25 % and wind speed often higher than 10 m/s. As stated, this is the direction along the fiord, with the air flow coming from the Kronebreen and Kongsvegen glaciers. The second most frequent direction observed at the CCT site during these seasons is from S-SW sectors, being this air flow coming from the Broggerbreen glaciers. The frequency of occurrence is usually less than 10 % but in summer (JJA) can reach 15 %. The wind speed usually range between 2.5 and 7.5 m/s. The third frequent wind sector, but with less than 10 % of the occurrences and speed generally lower than 5 m/s, is from N-W sector in direction of the open sea. In summer, these three wind sector distributions and wind speed become comparable, with corresponding decrease of occurrence from the E-SE sectors.

Table 2 summarizes the multi-year seasonal statistics for meteorological parameters measured at 2 m and evaluated from daily means.

3.3 Vertical atmospheric profiles

The CCT meteorological measurements set up can provide the vertical profiles of the atmospheric parameters. As an

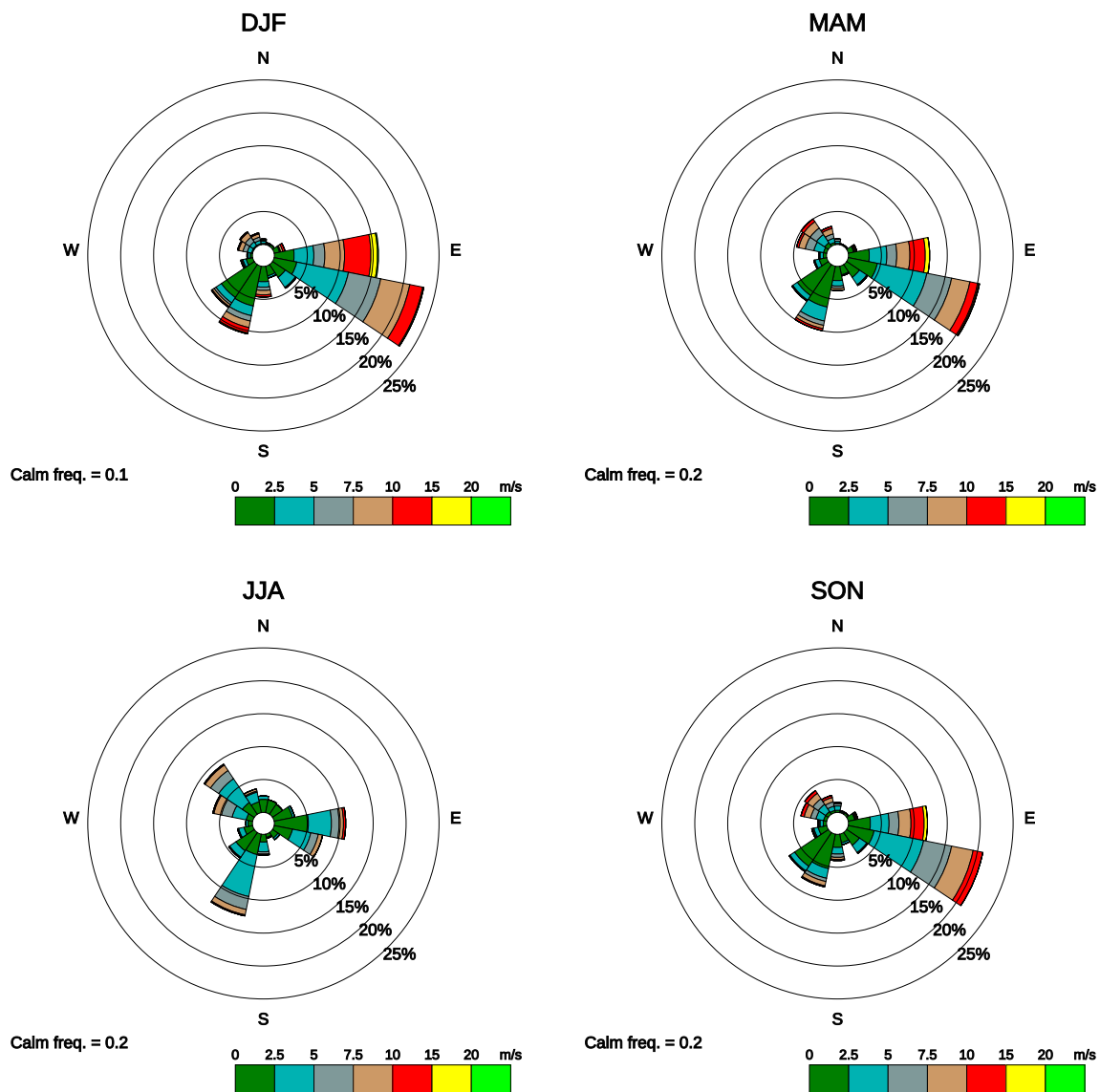


Fig. 3 Multi-year seasonal distributions of wind speed and direction measured at 10 m for the complete period under consideration

example of the variability of the atmospheric parameter with the height in Table 3 multi-year seasonal statistics for the differences between measurements at 33 and at 2 m are reported. The temperature data show the presence of ground-based inversion during all seasons, more pronounced during cold months, when solar heating is weak or absent. Differences higher than 2 °C (daily value) were found. Humidity is on average lower at 33 m with respect to 2 m (negative difference) with absolute values greater during summer. Wind speed presents a similar behavior of temperature, with positive gradients, more pronounced during cold seasons (max daily value ~ 4 m/s). For the wind differences between 33 and 2 m the cumulative monthly mean are only indicative of the variability with height. Accurate selective approach with respect to the

main flow must be applied to the data, for the parameterization of the ABL and reproduction of the wind profile for different atmospheric stability conditions.

3.4 Radiation measurements

The interannual variability of the short and long wave, incoming and outgoing, radiation components and the radiation balance based on the monthly averages and shown in Fig. 4. The maximum value of incoming SW as expected for June, with some variability due to the cloud coverage, ranged between 237 and 270 Wm⁻², for all the years except for the 2013. In this month the incoming SW reached the minimum value (211 Wm⁻²) even when compared to those of May 2011, 2012, 2014 and 2015 and

Table 2 Multi-year seasonal statistics for meteorological parameters measured at 2 m and evaluated from daily means. Percentiles are provided for temperature, specific humidity and wind speed

Season	Mean	St. Dev	Min	10th	25th	50th	75th	90th	Max
Temperature (°C)									
MAM	−6.4	5.7	−22.2	−14.6	−10.5	−5.9	−1.7	0.7	4.8
JJA	5.1	2.5	−1.6	1.6	3.5	5.3	6.8	7.9	13.7
SON	−2.8	5.7	−18.9	−10.9	−6.8	−2.6	1.8	4.1	7.5
DJF	−7.9	6.0	−24.4	−16.3	−12.5	−7.3	−3.0	−0.3	3.2
Specific humidity (g/kg)									
MAM	1.9	1.0	0.4	0.7	1.0	1.8	2.6	3.3	4.5
JJA	4.6	0.7	2.6	3.5	4.1	4.6	5.1	5.5	6.5
SON	2.7	1.3	0.3	1.1	1.6	2.6	3.7	4.5	5.7
DJF	1.7	1.0	0.2	0.6	0.9	1.6	2.4	3.1	4.3
Wind speed (m/s)									
MAM	3.2	2.4	0.3	1.0	1.4	2.5	4.2	6.4	14.8
JJA	2.6	1.5	0.4	1.0	1.5	2.2	3.3	4.7	8.5
SON	3.0	2.2	0.1	0.8	1.3	2.3	4.2	6.2	14.3
DJF	3.9	2.6	0.6	1.2	1.8	3.2	5.4	7.5	17.0
Wind direction (°)									
MAM	190.7	57.3	–	–	–	–	–	–	–
JJA	182.0	92.7	–	–	–	–	–	–	–
SON	186.8	57.6	–	–	–	–	–	–	–
DJF	178.2	49.9	–	–	–	–	–	–	–

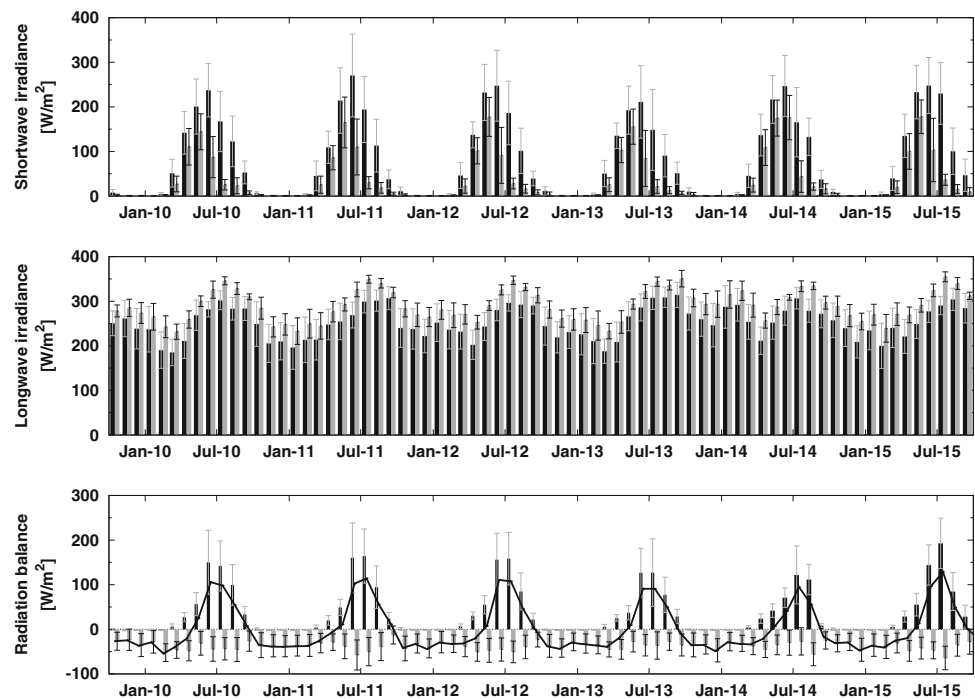
Table 3 As in Table 2 but for differences between values at 33 m and 2 m

Season	Mean	St. Dev	Min	10th	25th	50th	75th	90th	Max
Temperature (°C)									
MAM	0.8	0.4	0.1	0.4	0.5	0.8	1.1	1.4	2.3
JJA	0.2	0.4	−2.8	−0.1	0.0	0.2	0.4	0.7	2.6
SON	0.8	0.7	−9.5	0.3	0.5	0.8	1.1	1.3	1.9
DJF	0.9	0.4	−0.1	0.4	0.6	0.9	1.3	1.6	2.3
Specific humidity (g/kg)									
MAM	−0.04	0.06	−0.31	−0.12	−0.08	−0.03	0.01	0.03	0.13
JJA	−0.08	0.25	−0.33	−0.18	−0.14	−0.10	−0.06	0.00	0.29
SON	−0.04	0.14	−1.96	−0.12	−0.08	−0.03	0.02	0.05	0.19
DJF	−0.01	0.05	−0.18	−0.08	−0.04	−0.01	0.02	0.05	0.15
Wind speed (m/s)									
MAM	1.0	0.7	−0.1	0.3	0.4	0.8	1.3	2.0	3.7
JJA	0.6	0.6	−0.5	0.0	0.2	0.5	0.9	1.4	3.2
SON	0.9	0.7	−1.7	0.1	0.4	0.8	1.4	1.9	4.1
DJF	1.1	0.7	0.0	0.4	0.6	1.0	1.5	2.1	3.6
Wind direction (°)									
MAM	11.4	18.0	–	–	–	–	–	–	–
JJA	9.4	18.5	–	–	–	–	–	–	–
SON	12.4	19.2	–	–	–	–	–	–	–
DJF	9.1	11.8	–	–	–	–	–	–	–

July 2015 ($214 < SW < 233 \text{ Wm}^{-2}$). This change in July 2013 was probably due to an anomalous increase of cloudiness and even to the presence of fog in the low layers of the atmosphere of Kongsfjord. Detailed analysis of the

specific humidity data and could explain such a phenomenon. Due to the combination of rising of solar height and snow melting, the upwelling SW radiation values were higher during the months of April ($86\text{--}110 \text{ Wm}^{-2}$), May

Fig. 4 Monthly values with standard deviation of *top pane* the downwelling (*black bars*) and upwelling (*gray bars*) SW radiation; *middle panel* the downwelling (*black bars*) and upwelling (*gray bars*) LW radiation, and *bottom panel* SW balance (*black bars*), LW balance (*gray bars*) and total radiation balance (*black line*)



(144–177 Wm^{-2}) and June (84–176 Wm^{-2}). The maximum value of SW reflected component was measured on July 2014 due to the exceptional persistence of snow coverage.

The LW downwelling radiation presented the minimum values during the months of January, February and March (between 185 and 200 Wm^{-2}). The highest values for each year were during July and September (values between 296 and 314 Wm^{-2}). A similar yearly cycle characterizes the upwelling LW radiation: the minima were during the same months as for downwelling radiation (232–239 Wm^{-2}), while the maxima were during July, August and September (335–355 Wm^{-2}).

The SW radiation balance, defined as $SW_{\downarrow} - SW_{\uparrow}$, always positive, goes to zero when the Sun is not present and reaches the highest values during the months of June and July (102–135 Wm^{-2}). The LW balance, defined in a similar way, was always negative as expected for polar regions and presents minima during summer/spring (varying from -49 to -33 Wm^{-2}), and maxima during fall/winter (from -40 to -25 Wm^{-2}). The LW balance is related to cloud cover conditions (Dürr and Philipona 2004). During July 2013 this value was very low in absolute terms, confirming the persistence of cloudiness during this month.

The total radiative balance, sum of the two above, was positive only for the months between May and September, with the exception of 2012 and 2013 when it was slightly negative during this last month. Summer values were

between 86 and 91 Wm^{-2} . When there is no SW radiation the total balance coincides with the LW one and this reflects into the well-defined winter minima ($-42 \div -33$ Wm^{-2}).

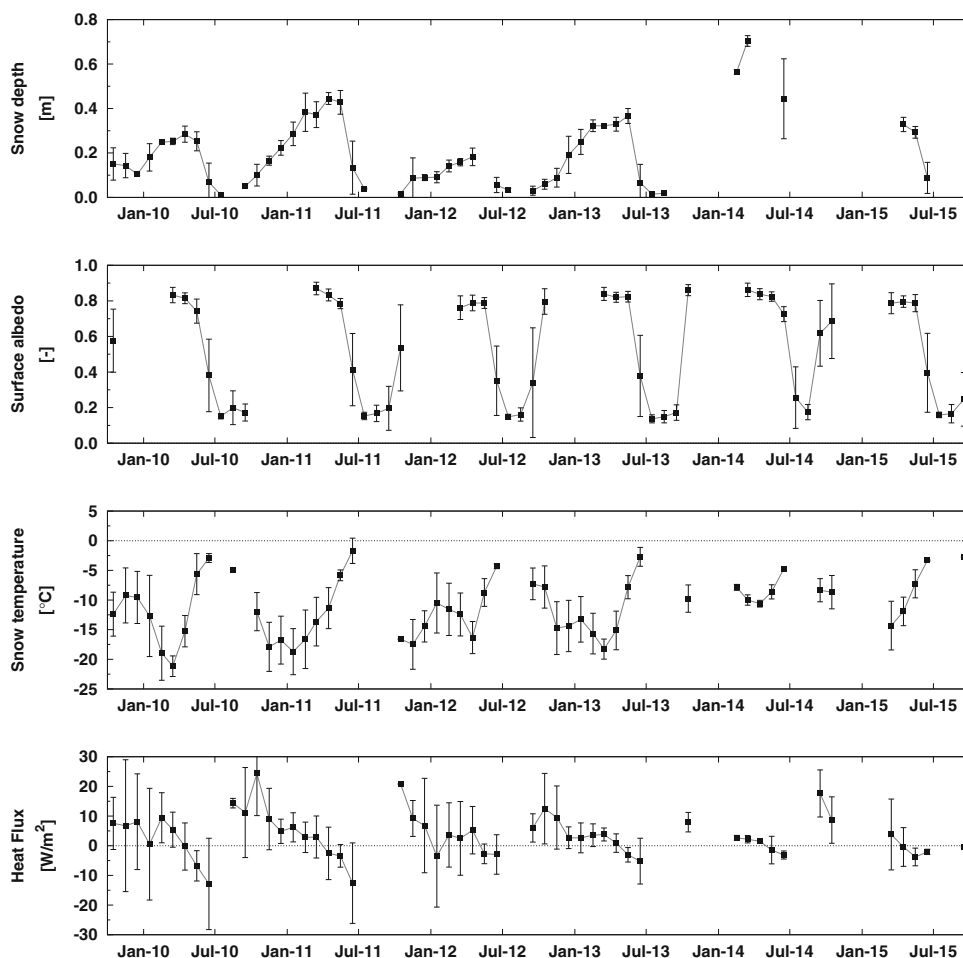
3.5 Characteristics of the snow coverage

One of the important components of the arctic climate system is the snow. Temperature, depth, melting period and duration are some of the characteristics of the snow layer to be taken into account when studying the energy and radiation balance at the surface, the turbulent fluxes, the albedo variability and the effect of surface coverage.

In Fig. 5, monthly mean values of the snow depth, measured by the SR50 sensor, the surface albedo, the snow temperature, measured by lower thermistors for snow depth >10 cm, and the heat flux between the soil and the snow layer are plotted. The albedo has been obtained by the CNR1 radiation measurements, for the period 2009–2015. In autumn 2013 and 2014 and in winter 2015 part of snow height data were missed because of sensor failure.

At the CCT site the snow depth reached a maximum of 0.7 m in March 2014, while the total accumulated snow (sum of the snowfall depths) was 1.02, 1.96, 1.34, and 1.60 m during the previous four winters. According to the measurements, the maximum temporal extension of the snow coverage (depth >5 cm) occurred between 20 September 2010 and 15 June 2011, for 265 days, while the minimum occurred between 24 November 2011 and 29

Fig. 5 Monthly values and standard deviation of snow depth (*first panel*), snow albedo (*second panel*), snow temperature (*third panel*) and snow-ground heat flux (*last panel*) over the complete period



June 2012, for 225 days. For the 2014 and 2015 the temporal extension is evaluable, but the snow depths went below the limit of 5 cm on 30th of June and on 8th of June, respectively.

An interesting feature concerning the snow melting season, when the snow depth decreased more than 1 cm/day, can be retrieved analyzing the snow depth variations. The snow melting season lasted between 6th and 11th June for 2010 (average melting rate of 2.8 cm/day), between 30th of May and 14th of June for 2011 (2.6 cm/day), between 1st and 7th of June for 2012 (3.0 cm/day), between 30th of May and 6th of June for 2013 (average of 3.8 cm/day), and between 19th of May and 10th of June on 2015 (1.9 cm/day).

The value of surface albedo in the observation area depends on the type surface coverage and is measurable only in presence of sufficient incoming SW radiation. Assuming the months of March and April as representative of the sunlight season with still snow coverage, the albedo averaged monthly values range between 0.76 and 0.87. On the other hand, in July and August the albedo represents

snow-free surface values varying between 0.14 and 0.20. October is a transition period, when sunlight is still present and the first snowfall occurs. In fact, the monthly averaged albedo in October varied from 0.49 to 0.81. During the melting season, the decrease of albedo daily values from 0.76 to 0.20 lasted 42 days in 2010, 61 in 2011, 29 in 2012, 21 in 2013 and 30 in 2015, showing an extreme year-to-year variability.

Snow temperature was evaluated only if snow depth is >10 cm, while heat flux if surface albedo >0.7 . The snow temperature showed strong day-to-day variations, between -10 and 10 °C, which are strongly linearly correlated with the air temperature. The heat flux between snow and ground was positive (heat from ground to snow) during fall and winter, from October to March with values up to 20 Wm^{-2} , and changes sign (heat from snow to ground) in April, May and June (when snow is present), with values down to -10 Wm^{-2} . The sign of heat flux between snow and soil depends on the moisture content of the soil itself (frozen or not) as stated in Bowles and O'Connell (1991).

4 Conclusions

The paper shows some peculiar characteristics of the environmental condition as observed by the instruments installed on the Amundsen-Nobile Climate Change Tower in Ny-Ålesund during the years 2009–2015. The data series are not enough to reveal some climatological trends, but are useful to study processes at different time scales of the measurement area. The particular position of the site allows to classify different meteorological conditions and relate the processes interaction at the air/soil/snow interface. Moreover, the CCT is a unique structure capable of providing continuous vertical profiles of the physical, meteorological and micro-meteorological parameters of the atmosphere. Studies on the correlation and interaction between these quantities, the surface conditions and radiation balance are ongoing. Studies on the vertical profiles of turbulence will be able to verify the validity of theories as well as explain processes concerning the flux of energy and mass from and to the atmosphere. Low level atmospheric circulation will be better classified and processes related to the interaction with long-range transport could be better explained.

In the frame of the project, the CCT represents a reference point for other scientific settings in the area. A clean grid area to continuous monitor of the permafrost layer and coverage of the surface upon the seasons has been set up close to the tower. The strong relationship between these components of the climate system will be investigated, in terms of variability of the surface coverage (snow and vegetation) local production of trace gases, atmospheric circulation, and radiation balance. A data system has been set up to manage, store and access the data. The Italian Arctic Data Center (IADC, <http://arcticnode.dta.cnr.it/cnr/>) aims to manage all the different data with capability to discover, visualize and download selected dataset.

An important contribution by CCT has been given in terms of increased international cooperation and the participation to important European projects as, e.g., SIOS (Svalbard Integrated Earth Observing System), Arctic UNION, EU-Polarnet. Deep and further analysis must be provided to explain all the interrelations between the processes in the Arctic climatic system, based also on the results that can be achieved at Ny-Ålesund by CCT measurements.

Acknowledgments This work was realized in the frame of the Climate Change Tower – Integrated Project of Dipartimento Scienze del Sistema Terra e Tecnologie per l’Ambiente-National Research Council of Italy, that supported the construction of the Amundsen Nobile CCT. The project was partially financed as National Interest Project by the Italian Minister of Education, University and Research (PRIN 2007 and PRIN 2009) and by Minister of Foreign Affairs (Bilateral project Italy-Korea). The authors wish to thank Dr. Taejin

Choi of KOPRI for the collaborative research active in Ny-Ålesund at CCT. Thanks are also due to personnel managing the facilities at the Dirigibile Italia Arctic Station. Authors acknowledge also Norwegian Polar Institute, Alfred-Wegener Institute and Kings Bay AS, for the help in using the facilities in Ny-Ålesund.

References

- Argentini S, Serraval R, Viola A, Mastrantonio G, Lupkes C, Petenko I, Pirazzini R (2000) Proc. 14th symposium on boundary layer and turbulence (Snowmass Village, Aspen, CO, 7–11 August 2000) pp. 602–605
- Beine HJ, Argentini S, Maurizi A, Mastrantonio G, Viola A (2001) The local wind field at Ny-Ålesund and the Zeppelin mountain at Svalbard. *Meteorol Atmospher Phys* 78(1–2):107–113. doi:10.1007/s007030170009. URL: <http://dx.doi.org/10.1007/s007030170009>
- Boville BA, Gent PR (1998) The NCAR Climate System Model, version one. *Journal of Climate* 11(6):1115–1130. doi:10.1175/1520-0442(1998)0111115:TNCSTMV2.0.CO;2
- Bowles D, O’Connell P (1991) Recent advances in the modeling of hydrologic systems. Kluwer Academic Publishers, Nato ASI series
- Curry JA, Schramm JL, Ebert EE (1995) Sea ice-albedo climate feedback mechanism. *J Clim* 8(2):240–247. doi:10.1175/1520-0442. URL:[http://dx.doi.org/10.1175/1520-0442\(1995\)0080240](http://dx.doi.org/10.1175/1520-0442(1995)0080240)
- Dürr B, Philipona R (2004) Automatic cloud amount detection by surface longwave downward radiation measurements. *J Geophys Res Atmos* 109:D5, n/a–n/a. doi:10.1029/2003JD004182. URL: <http://dx.doi.org/10.1029/2003JD004182.D05201>
- Eirik JFE, Benestad R, Hanssen-Bauer I, Haugen J, Engen-Skaugen T (2011) Temperature and precipitation development at Svalbard 19002100. *Adv Meteorol*. doi:10.1155/2011/893790
- Hartmann J, Albers F, Argentini S, Bochart A, Bonafe U, Cohrs W, Conidi A, Freese D, Georgiadis T, Ippoliti A, Kaleschke L, Lüpkes C, Maixner U, Mastrantonio G, Ravegnani F, Reuter A, Trivellone G, Viola A (1999) Arctic radiation and turbulence interaction study (artist). *Berichte zur Polarforschung* (Reports on Polar Research) Alfred Wegener Institute for Polar and Marine Research, Bremerhaven 305
- Lindsay R, Zhang J (2005) The thinning of arctic sea ice, 19882003: Have we passed a tipping point? *J Clim* 18:4879–4894. doi:10.1175/JCLI3587.1
- Maturilli M, Herber A, König-Langlo G (2015) Surface radiation climatology for Ny-Ålesund, Svalbard (78.9 n), basic observations for trend detection. *Theor Appl Climatol* 120(1–2): 331–339. doi:10.1007/s00704-014-1173-4
- Maturilli M, Herber A, König-Langlo G (2013) Climatology and time series of surface meteorology in Ny-Ålesund, Svalbard. *Earth Syst Sci Data* 5(1):155–163. doi:10.5194/essd-5-155-2013. URL:<http://www.earth-syst-sci-data.net/5/155/2013/>
- Mazzola M, Tampieri F, Viola A, Lanconelli C, Choi T (2016) Stable boundary layer vertical scales in the Arctic: observations and analyses at Ny-Ålesund, Svalbard. *Q J R Meteorol Soc* 142:1250–1258. doi:10.1002/qj.2727
- Moritz RE, Bitz CM, Steig EJ (2002) Dynamics of recent climate change in the arctic. *Science* 297(5586):1497–1502. doi:10.1126/science.1076522. URL:<http://science.sciencemag.org/content/297/5586/1497>
- Overland JE, Guest PS (1991) The arctic snow and air temperature budget over sea ice during winter. *J Geophys Res Oceans* 96(C3):4651–4662. doi:10.1029/90JC02264. URL: <http://dx.doi.org/10.1029/90JC02264>

- Screen JA, Simmonds I (2010) The central role of diminishing sea ice in recent arctic temperature amplification. *Nature* 464(7293):1334–1337. doi:10.1038/nature09051. URL: <http://dx.doi.org/10.1038/nature09051>
- Serreze MC, Barrett AP, Stroeve JC, Kindig DN, Holland MM (2009) The emergence of surface-based Arctic amplification. *Cryosphere* 3(1):11–19. doi: 10.5194/tc-3-11-2009. URL: <http://www.the-cryosphere.net/3/11/2009/>
- Stroeve J, Holland MM, Meier W, Scambos T, Serreze M (2007) Arctic sea ice decline: faster than forecast. *Geophys Res Lett* 34(9), L09,501 (2007). doi:10.1029/2007GL029703. URL: <http://dx.doi.org/10.1029/2007GL029703>
- Tampieri F, Viola A, Mazzola M, Pelliccioni A (2016) On turbulence characteristics at Ny-Ålesund—Svalbard. *Rend Fis Acc Lincei* (this issue)